Electrochemistry Communications 13 (2011) 1533–1535

Contents lists available at SciVerse ScienceDirect

Electrochemistry Communications

journal homepage: www.elsevier.com/locate/elecom

Coupling of a high throughput microelectrochemical cell with online multielemental trace analysis by ICP-MS

Sebastian O. Klemm [a,*], Angel A. Topalov [a,b], Claudius A. Laska [a], Karl J.J. Mayrhofer [a,*]

[a] Department of Interface Chemistry and Surface Engineering, Max-Planck-Institut für Eisenforschung, Max-Planck-Straße 1, 40 237 Düsseldorf, Germany
[b] Center for Electrochemical Sciences, Ruhr-Universität Bochum, Universitätsstraße 150, 44780 Bochum, Germany

ARTICLE INFO

Article history:
Received 15 September 2011
Received in revised form 14 October 2011
Accepted 17 October 2011
Available online 22 October 2011

Keywords:
Online electrolyte analysis
Copper dissolution
Inductively coupled plasma-mass spectrometry
Micro electrochemistry

ABSTRACT

In this work, the successful coupling of a specially designed microelectrochemical cell and direct online multi-elemental trace analysis by ICP-MS is presented. The feasibility of this method is demonstrated by the example of copper dissolution in HCl (1 and 10 mM), showing very high sensitivity and an excellent congruency between electrochemical experiments and copper concentrations detected downstream. The complementary data allows for a precise determination of the valence of Cu ions released during anodic dissolution, which undergoes changes depending on the electrolyte and the applied current density. Moreover it provides a means of quantification of processes without net external currents that are not readily accessible by plain electrochemical techniques, in particular the exchange current densities at the open circuit potential, i.e. corrosion rate, and the dissolution of native oxides. The system presented combines full spectrum electrochemical capabilities, convection control, and highly sensitive electrolyte analysis in an integrated, miniaturized arrangement under full computer control and automation.

1. Introduction

The online detection of dissolved species is of tremendous profit for many electrochemical investigations. It provides a distinction between the dissolved and precipitated form of ions, and allows associating the overall net current to the dissolution of specific elements in multi-component systems [1]. The advantages of this coupling have been outlined by several authors [2–5], utilizing various methods of downstream detection. ICP-MS in particular is one of the most sensitive and versatile analytical methods for most elements currently available. Very low detection limits and wide linear quantification ranges suit very well for electrochemical reactions, and the continuous mode of operation appears ideal for time resolved trace analysis.

Moreover, the high sensitivity allows reducing the size of the electrode area, and consequently enables the use of microelectrochemical cells [6,7]. Among those, capillary cells operated in contact mode offer the advantage of minimum requirements concerning sample geometry and preparation, and provide high reproducibility when an array of measurement locations is automatically addressed [8,9]. However, the severe cell geometry restrictions in capillaries introduce an undesired complexity to the flow profile if operated under electrolyte convection [4], which may lead to undefined mass transport and inhomogeneous current density distribution. The search for an optimized experimental integration of online element analysis in electrochemical measurements is thus still ongoing.

In the present study, we present a new technique that addresses the key challenges of coupling of a microelectrochemical cell with online multielemental trace analysis, and that additionally provides the basis for high throughput automation. The core development is an acrylic block scanning flow cell (SFC) containing channels in V-geometry. This cell concertedly enables (i) facile coupling with an online analysis system such as an ICP-MS; (ii) integration in an XYZ-positioning system that allows quick and easy sample exchange; (iii) high-throughput experimentation by full computer controlled measurement execution on various locations; and (iv) controlling the flow profile in the electrochemical cell by the channel geometry and working electrode opening, readily changed by standard mechanical machining. The exact knowledge of the inner geometry of the cell and the well controllable flow rates furthermore allow the use of fluid simulations to predict the flow profile on the surface and to optimize the cell geometry to meet specific mass transport requirements.

For an initial system characterization, the dissolution of copper in HCl solution was chosen because of the coexistence of spontaneous dissolution (corrosion) and induced dissolution upon anodic polarization. In this preliminary work particular focus is set on the correlation between applied electrochemical current and measured dissolution current as calculated by the flux of copper ions entering the online analytics, which demonstrates the great potential of the combined technique.

* Corresponding authors. Tel.: +49 211 6792 160; fax: +49 211 6792 218.
E-mail addresses: klemm@mpie.de (S.O. Klemm), mayrhofer@mpie.de (K.J.J. Mayrhofer).

1388-2481/$ – see front matter © 2011 Elsevier B.V. All rights reserved.
doi:10.1016/j.elecom.2011.10.017

2. Experimental

The microelectrochemical scanning flow cell (SFC) is schematically shown in Fig. 1, including tubing (Tygon®, 380 µm inner diameter, 2 mm outer diameter), counter electrode (four 25 µm platinum wires, 99.99%), and reference (µ-Ag/AgCl [10], Agar solidified 1 M KCl, Potential 215 mV vs. SHE). The contact area to the substrate (0.256 mm^2) was confined by a silicone gasket (RTV 118Q, Momentive) manually applied to the tip. The dimensions given were found optimal for mechanical preparation of the tip. A reduction of the inner channel diameter to 200 µm would yield stable flow rates and robust sample contact as well [5] given the required precision during the manufacturing process. Due to the use of peristaltic pumps and the flow rate requirements of the ICP-MS, further reduction of the cell size could prove very difficult.

The microcell was mounted on a force sensor (KD45 2 N, ME-Messsysteme) that adjusts the force to 300 ± 5 mN in contact mode. The sample positioning is achieved by a YXZ-translation stage (3× M-403.6 DG, Physik Instrumente). An in-house developed LabVIEW program controls all components simultaneously [9].

Electrochemical measurements were performed with a potentiostat (Gamry Reference 600) controlled by in-house programmed LabVIEW routines. 10 and 1 mM HCl electrolytes were prepared from Suprapur® HCl (Merck) and ultrapure water (PureLab Plus system, Elga). The substrate material was a 0.5 mm copper foil (99.99%), ground with Si:C grinding paper and polished with a 3 µm diamond suspension.

The electrolyte pumped through the microcell and over the working electrode is subsequently introduced into the ICP-MS system (NexION 300X, Perkin Elmer), equipped with a cyclonic spray chamber and a Meinhard nebulizer. The RF power for the plasma was held at 1300 W with a gas flow of 15 L min^{-1}. Transient signals of ^{63}Cu, ^{65}Cu and the internal standard ^{89}Y (5 ppb, mixing ratio between analyte and standard 1:4), were recorded in parallel with a dwell time of 100 ms and 5 sweeps per reading. The detected intensities were analyzed with respect to the internal standard, which helps to compensate for instrument dependent fluctuations of the mass signals over time. ICP-MS calibration was performed prior to each measurement.

3. Results and discussion

The experiments with the SFC coupled to the ICP-MS were typically performed under continuous electrolyte flow by (i) pressing the microcell on the working electrode substrate, (ii) conducting an experimental sequence, (iii) cell liftoff, and (iv) moving to another location above the sample for the next investigation. During the whole procedure, the ICP-MS records the concentration of relevant elements. Fig. 2 shows two independent experimental runs on different locations on a Cu sample using 1 mM HCl as electrolyte. The sample was held at the open circuit potential (OCP), interrupted by a sequence of applied current steps of 200 s each, with spacing of 300 s. The copper concentrations recorded online can be transferred into a dissolution current by multiplication with the charge number z, the volume flow rate V_f and the Faraday constant:

$$I_{Diss} = z \cdot F \cdot V_f \cdot c_{Cu}. \quad (1)$$

With a charge number of 1 (Cu^+) [3,11] and a volume flow of 51 µL min^{-1}, the conversion factor between concentration and current equals 82.01 nA/µmol L^{-1}.

Data plotting is arranged in an XYY-diagram where the left axis shows the calculated dissolution current determined by the ICP-MS according to Eq. (1), while the right axis corresponds to the galvanic dissolution current as the sum of the spontaneous dissolution and the applied current. This applied current during specific intervals is superimposed on a linear fit of the baseline that originates from the spontaneous Cu dissolution at the open circuit potential.

The events of contacting the substrate (t = 0 s) and microcell liftoff (t = 3800 s for run 1, t = 4000 s for run 2) are well reflected in the dissolution profile. The inset illustrates the dead time required for species to reach the detector, and the initial copper peak before the signal reaches steady state. Numeric integration of both peaks with respect to the corrosion current (dotted line) yields a total amount of dissolved copper equal to 58 pM and 70 pM. It appears likely that this peak originates from the dissolution of the native oxide upon electrolyte contact. With a wetted area of 0.256 mm^2 and the molar mass and density for cupric oxide (Cu_2O, M = 143.14 g mol^{-1}, ρ = 6.0 g cm^{-3} [12]), the peak integral corresponds to a native oxide thickness of 5.4 and 6.5 nm, respectively. The slight deviation observed between both replicates is most likely due to a non-uniform native oxide; the estimated thicknesses however appear reasonable [13].

After the initial dissolution of the native oxide within the first 120 s, the Cu surface reaches an equilibrium state with an OCP of approximately 245 ± 5 mV_{SHE} and an almost constant corrosion current of 25 nA (9.8 µA cm^{-2}). This value appears reasonable in comparison to other studies in hydrochloric acid of various concentrations [14]. The slight decline of the corrosion rate during the experiment was also confirmed in the absence of galvanostatic steps in other experimental series. Inspection of the electrode surface after prolonged

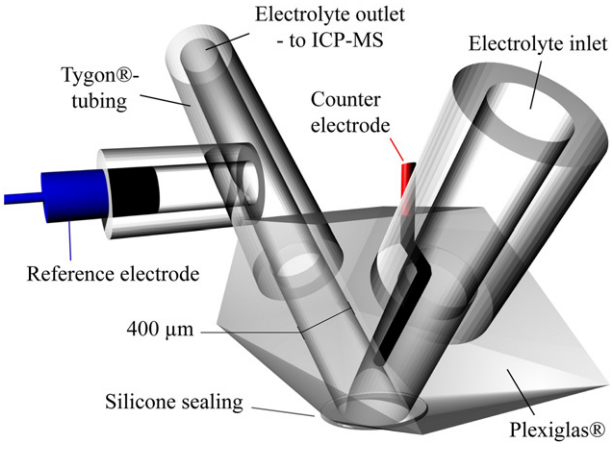

Fig. 1. 3D-illustration of the microcell geometry with labeled components. Scaling modified for clarity.

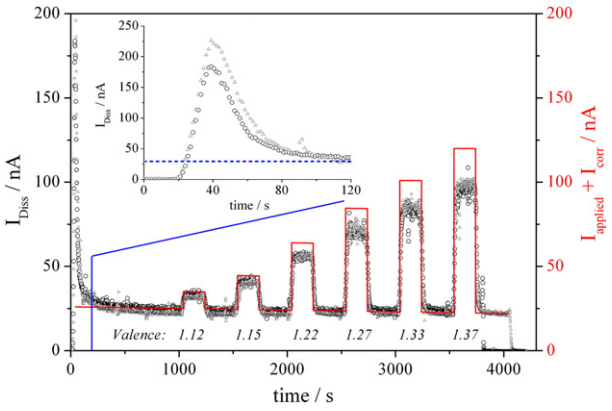

Fig. 2. Copper dissolution current profile for two independent replicates (I_{Diss}, hollow spheres and triangles, left axis) and overlaid sum of applied current and corrosion current ($I_{Corr} + I_{applied}$, red line, right axis) in aerated 1 mM HCl under electrolyte flow (51 µL min^{-1}) at room temperature. The inset shows the magnified initial region with indication of the baseline (dashed line, I_{Corr}) and the dissolution valence displayed is the quotient of applied current and mean plateau dissolution current.

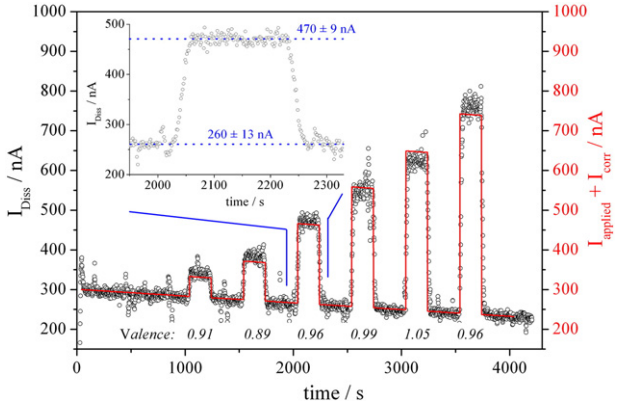

Fig. 3. Copper dissolution current profile (I_{Diss}, hollow spheres, left axis) and overlaid sum of applied current and corrosion current ($I_{Corr} + I_{applied}$, red line, right axis) in aerated 10 mM HCl under electrolyte flow (51 μL min^{-1}) at room temperature. The inset shows the magnified region between 1950 and 2330 s with linear approximation of the plateau values for the baseline and during galvanostatically applied current (100 nA). The dissolution valence is the quotient of applied current and mean plateau dissolution current.

exposition to the corrosive medium showed an altered surface morphology, essentially being strongly roughened. This change in surface morphology is most likely responsible for the transient corrosion rate under OCP conditions in the microcell measurements.

When an anodic current is applied to the working electrode, additional Cu dissolves into the electrolyte. Fig. 2 demonstrates the correlation between the amount of Cu detected downstream and the one expected from the several current pulses (200 s) with increasing intensity. In a first approximation, excellent overlap between the onset, plateau height and decline of the dissolution current with the galvanic experiment is achieved. However, a quite substantial deviation in the magnitudes occurs especially at higher dissolution rates. To further investigate this surprising effect, the conditions were modified by increasing the acid (and consequently chloride) concentration to 10 mM under otherwise constant settings; the results are shown in Fig. 3.

The corrosion rate of copper in 10 mM HCl (250–300 nA, 97.6–117.1 μA cm^{-2}) at open circuit conditions is significantly higher than in Fig. 2. In fact, the difference in corrosion current (factor of 10) appears to accurately reflect the dilution ratio between 1 and 10 mM HCl, showing the sensitivity for the chloride concentration and pH. A steeper decrease of the corrosion rate at OCP compared to 1 mM HCl is due to the significantly stronger alteration of the surface morphology during the measurement.

For the superimposed galvanic sequence, here consisting of 200 s current pulses of 100 to 500 nA, again an excellent agreement between dissolution and applied current is observed. The transition regions between the OCP-measurement and applied currents are sharp, also evident from the magnified inset of Fig. 3. Approximately 20 s is required for the signal to reach 80% of its final value. The inset further highlights that the magnitude of applied current (200 nA) is accurately reflected by the difference in the plateau regions of the dissolution current (dotted lines), showing that the assumption of Cu dissolving with a valence of one is principally correct. This is, however, not true for the experiments in 1 mM HCl, where the apparent dissolution valence increases with higher applied currents. Obviously, under such conditions Cu dissolves partly as mono- and bivalent ion, the ratio of which is strongly depending on the current density. This finding is in agreement with the dissolution mechanism proposed by Jardy et al., stating that an increasing surface activity of Cu(I) triggers the disproportionation reaction and consequently an increase of the dissolution valence [15,16]. Further experiments will be necessary to completely grasp the effect; however, these initial measurements already provide a first indication for its extent.

4. Conclusions

The coupling between SFC and ICP-MS is a new promising approach as it combines high throughput capabilities with an exceptionally high sensitivity for online multi element analytics. The special cell geometry presented is characterized by a very low internal volume (~5 μL microcell, ~21 μL tubing), a decreased dead time (30 s at 51 μL min^{-1}), and a small wetted area of $2.56 \cdot 10^{-3}$ cm^2. The parallel recording of electrochemical and dissolution data performed on the example of copper dissolution in diluted HCl immediately allows to determine the dissolution valence of ions, which is highly dependent on the applied current density and the electrolyte. Moreover, current-less dissolution processes, like the corrosion rate at the corrosion potential and the dissolution of native oxides, can be directly monitored. The broad spectrum of possible analytes and small demands concerning sample type, preparation, and geometry allow for an exceptionally wide field of application.

Acknowledgments

We kindly acknowledge the experimental assistance provided by Andrea Mingers and the financial support by IMPRS-SurMat.

References

[1] M. Mokaddem, P. Volovitch, K. Ogle, Electrochimica Acta 55 (2010) 7867.
[2] J.O.M. Bockris, B.T. Rubin, A. Despic, B. Lovrecek, Electrochimica Acta 17 (1972) 973.
[3] K. Ogle, S. Weber, Journal of the Electrochemical Society 147 (2000) 1770.
[4] N. Homazava, A. Ulrich, M. Trottmann, U. Krahenbuhl, Journal of Analytical Atomic Spectrometry 22 (2007) 1122.
[5] S.O. Klemm, S.E. Pust, A.W. Hassel, J. Hüpkes, K.J.J. Mayrhofer, Journal of Solid State Electrochemistry (2011) 1.
[6] T. Suter, H. Bohni, Electrochimica Acta 42 (1997) 3275.
[7] M. Sánchez, J. Gamby, H. Perrot, D. Rose, V. Vivier, Electrochemistry Communications 12 (2010) 1230.
[8] M.M. Lohrengel, A. Moehring, M. Pilaski, Electrochimica Acta 47 (2001) 137.
[9] S.O. Klemm, J.-C. Schauer, B. Schuhmacher, A.W. Hassel, Electrochimica Acta 56 (2011) 4315.
[10] A.W. Hassel, K. Fushimi, M. Seo, Electrochemistry Communications 1 (1999) 180.
[11] G. Kear, B.D. Barker, F.C. Walsh, Corrosion Science 46 (2004) 109.
[12] H.A. Miley, Journal of the American Chemical Society 59 (1937) 2626.
[13] S. Suzuki, Y. Ishikawa, M. Isshiki, Y. Waseda, Materials Transactions, JIM 38 (1997) 1004.
[14] W.H. Smyrl, L.L. Stephenson, Journal of the Electrochemical Society 132 (1985) 1563.
[15] A. Jardy, A.L. Lasallemolin, M. Keddam, H. Takenouti, Electrochimica Acta 37 (1992) 2195.
[16] B. Yuan, C. Wang, L. Li, S. Chen, Electrochemistry Communications 11 (2009) 1373.